eJSE International

Special Issue: Electronic Journal of Structural Engineering 14(1) 2015

Damage Detection of Circular Cylindrical Shells by Ritz Method and Wavelet Analysis

L. Sarker, Y. Xiang, X.Q. Zhu & Y.Y. Zhang

School of Computing, Engineering and Mathematics, University of Western Sydney, Sydney, Australia

Email: xinqun.zhu@uws.edu.au

ABSTRACT: This paper presents a new technique based on the Ritz method for the damage detection of circular cylindrical shell structures. Sander's thin shell theory together with the Ritz method is used to analyse the dynamic behaviour of circular cylindrical shells. The crack damage on the shell surface is modelled by a rotational line spring along the circumference of the shell. Different damage scenarios are investigated by changing the crack locations and rotational spring stiffness. Modal parameters of shells with different damage patterns are obtained and compared. Wavelet analysis is carried out to detect the discontinuities in the mode shape where the damage is presented. It is found from the numerical results that the natural frequencies of the shell are insensitive to the crack damage. The wavelet analysis is effective to detect the damage in the circular cylindrical shell.

Keywords: Circular cylindrical shell, Damage detection, Ritz method, Wavelet analysis

1 INTRODUCTION

Cylindrical shells are widely used in various engineering fields as key structural components such as pressure vessels, storage tanks, pipes, water ducts and process equipments. Loading and environmental attack lead to the accumulation of damages in structures. In order to avoid disastrous structural failures induced by damages, it is essential to detect the damage in the very early stage of damage propagation. In general, damage will result in a local reduction in stiffness which in turn changes the dynamic behaviour of the structure, including natural frequencies, mode shapes and damping ratios. Numerous research studies have been conducted to use the change of structural vibration properties for damage detection. Doebling et al. (1998), Sohn et al. (2000) and Brownjohn (2007) presented the literature review on damage detection based on parameters such as natural frequencies, mode shapes, mode shape curvatures, flexibility matrix and stiffness matrix. However, most of the researchers used beam or plate structures in their damage detection modelling, and only a few studies were based on shell structures.

Generally, a crack in a structure introduces local flexibility which usually changes the dynamic behaviour of the structure that can be used as a possible means to detect the crack. Rice and Levy (1972) modelled the crack as a line spring model. The spring stiffness is related to a specific crack depth and severity and determined by a localised flexibility matrix based on fracture mechanics. This model is widely used to analyse the dynamic behaviour of beam and plate structures with cracks. However, few works have been done on shell structures. In one of the few studies, Roytman and Titova (2002) developed an analytical mathematical model to analyse the elastic oscillations of a cylindrical shell with surface closing cracks. Relay's energy conservation method was employed to derive the governing equation of motion for the system. Analytical solutions were obtained by using Fourier transformation method. The effect of the crack shape, such as square, triangle, or spherical was discussed. Javidruzi et al. (2004) conducted finite element analysis on the vibration, buckling and dynamic stability of cracked cylindrical shells. The effect of crack length and orientation on the vibration frequency of a cracked cylindrical shell was investigated. A numerical analysis of partially cracked cylindrical shell system was performed by Mohan (1998) using the finite element analysis software ABAQUS. The line spring model was used to simulate the par-

tial crack in the shell structure. The line-spring crack model essentially reduces a complex three dimensional cracked shell system problem into a two dimensional one by transforming the crack mechanism into a series of line spring connections. It was also observed in their study that the results are closer to the experimental ones than that by other models. Lee et al. (2006) presented a structural damage identification method based on frequency response function (FRF) data. Their method was very efficient since it only required FRF data at damaged state. Zhu et al. (2007) analyzed the vibrational power flow of an infinite cylindrical shell with a circumferential surface crack. The surface crack was modelled using the equivalent distributed line spring. Their results showed that due to the presence of the crack the vibrational power flow changes dramatically and the change is strongly dependent on the depth and position of the crack. Sarker et al. (2011) used Ritz method to analyze the vibration of cylinder shell with cracks and detected cracks by using the second derivative of mode shape. Zhang et al. (2014) presented a damage detection method based on frequency shift curve for cylindrical shell structures.

Wavelet analysis has attracted enormous attention from researchers due to its ability to analyze non-stationary signals such as the damage signal in structures. Wavelet analysis can be implemented successfully to detect the changes occurred in the mother signal as a means for damage detection. It can also be used to separate the noise from the original signal to extract the data which may be hidden by the noise. A wavelet based approach for structural damage detection of beams, plates and composite plates was proposed by Rajasekaran and Varghese (2005). By breaking the dynamic signal of the structural response into a series of local basis functions (also called wavelets) and using its scaling and transformation property, the special characteristic of the structure can be identified. A structural damage detection method based on wavelet transform was proposed by Lu and Hsu (2002) where they compared the vibration signals from the intact and damaged structures after the discrete wavelet transform. The presence, position and number of damages in the structure were determined. The defects in the structure were simulated by attaching several point masses and spring on the string. They observed from the numerical results that even the minor changes in the structure have effects in the wavelet coefficients of the vibration signals. Law et al. (2005) showed analytically the relationship between the local change in the system parameters and the sensitivity of the wavelet packet transform component energy in a dynamic system. Their results showed that the method is insensitive to measurement noise and can define the damages at close proximity. Initial damage of composite laminated plates based on the energy variation of the structural dynamic response was investigated by Yan and Yam (2002). They implemented the online damage detection method and used wavelet analysis to determine the dynamic response of the plates. The constructed damage index changed with the propagation of the crack and the method was also very sensitive to small damage (Yan et al. 2007).

In this study we investigate the dynamic behaviour of a circular cylindrical shell with circumferential surface crack by using the Ritz method. The surface crack is modelled as the line spring that provides the continuity among the internal forces. Different damage scenarios are simulated by changing the crack locations and spring stiffness. Modal parameters of the shells with different damages are obtained and compared. Wavelet analysis is carried out to detect the discontinuities in the mode shape where the damage is presented. The location and extent of the damage are predicted by the changes of modal parameters. Simulation results show that the proposed method is effective and accurate to determine the crack damage in the cylindrical shell structures, indicating the potential applications of the method in damages detection for oil pipelines and other cylindrical shell-type structures.

2 VIBRATION ANALYSIS OF SHELLS BY RITZ METHOD

Consider a circular cylindrical thin shell of uniform thickness h, radius R, length L, mass density ρ, modulus of elasticity E, Poisson's ratio ν, and shear modulus $G = E/[2(1+\nu)]$. The geometry and coordinate system of the shell is shown in Figure 1.

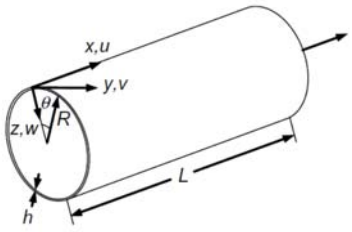

Figure 1. Geometry of a cylindrical shell.

Based on Sander's thin shell theory, the strain energy U of bending and stretching of the cylindrical shell is given by (Leissa, 1973)

$$U=\int_0^L\int_0^{2\pi}\left\{\frac{Eh}{2(1-\nu^2)}\left[\left(\frac{\partial u}{\partial x}\right)^2+\frac{1}{R^2}\left(\frac{\partial v}{\partial\theta}+w\right)^2+\frac{2\nu}{R}\left(\frac{\partial u}{\partial x}\right)\left(\frac{\partial v}{\partial x}+w\right)+\frac{1-\nu}{2}\left(\frac{\partial v}{\partial x}+\frac{1}{R}\frac{\partial u}{\partial\theta}\right)^2\right]\right.$$
$$+\frac{Eh^3}{24(1-\nu^2)}\left[\left(\frac{\partial^2 w}{\partial x^2}\right)^2+\frac{1}{R^4}\left(\frac{\partial^2 w}{\partial\theta^2}-\frac{\partial v}{\partial\theta}\right)^2+\frac{2\nu}{R^2}\left(\frac{\partial^2 w}{\partial x^2}\right)\left(\frac{\partial^2 w}{\partial\theta^2}-\frac{\partial v}{\partial\theta}\right)\right.$$
$$\left.\left.+\frac{2(1-\nu)}{R^2}\left(-\frac{\partial^2 w}{\partial x\partial\theta}+\frac{3}{4}\frac{\partial v}{\partial x}-\frac{1}{4R}\frac{\partial u}{\partial\theta}\right)^2\right]\right\}Rd\theta dx \quad (1)$$

where *u, v, w* are displacements in the longitudinal, tangential, and radial directions; *x* and θ are longitudinal and circumferential coordinates, respectively. Neglecting the effect of rotary inertia since only the thin shell is considered, the kinetic energy *T* of the cylindrical shell is given by

$$T=\int_0^L\int_0^{2\pi}\left\{\frac{1}{2}\rho h\left[\left(\frac{\partial u}{\partial t}\right)^2+\left(\frac{\partial v}{\partial t}\right)^2+\left(\frac{\partial w}{\partial t}\right)^2\right]\right\}Rd\theta dx \quad (2)$$

The Lagrangian functional *F* is the sum of the strain and the kinetic energies of the shell

$$F=U+T \quad (3)$$

Assuming harmonic vibration, the following functions are adopted to separate the spatial variables *x*, $\theta$and the time variable *t*:

$$u(x,\theta,t)=U(x)\sin n\theta e^{i\omega t}$$
$$x(x,\theta,t)=V(x)\cos n\theta e^{i\omega t}$$
$$w(x,\theta,t)=W(x)\sin n\theta e^{i\omega t} \quad (4)$$

where *n* is the number of circumferential waves and ω is the circular frequency of vibration.

By substituting Eq. (4) into Eq. (3), the Lagrangian functional can be expressed as

$$F=\frac{EhR\pi e^{2i\omega t}}{2(1-\nu^2)}\int_0^L\left\{\left[\left(\frac{dU}{dx}\right)^2+\frac{1}{R^2}(nV-W)^2-\frac{2\nu}{R}\left(\frac{dU}{dx}\right)(nV-W)+\frac{1-\nu}{2}\left(\frac{dV}{dx}+\frac{nU}{R}\right)^2\right]\right.$$
$$+\frac{h^2}{12}\left[\left(\frac{d^2W}{dx^2}\right)^2+\frac{1}{R^4}(n^2W-nV)^2+\frac{2\nu}{R^2}\left(\frac{d^2W}{dx^2}\right)(n^2W-nV)\right.$$
$$\left.\left.+\frac{2(1-\nu)}{R^2}(-n\frac{dW}{dx}+\frac{3}{4}\frac{dV}{dx}-\frac{nU}{4R})^2\right]\right.$$
$$\left.-\omega^2\rho h(U^2+V^2+W^2)\right\}dx \quad (5)$$

2.1. Geometric boundary conditions

For simply supported cylindrical shells, Sobel (1964) identified four kinds of boundary conditions that are designated as follows:

$$S_1: W=V=0; S_2: W=0; S_3: W=U=0; S_4: W=U=V=0 \quad (6)$$

Similarly for clamped shells, the boundary conditions are

$$C_1: W=\frac{dW}{dx}=V=0; C_2: W=\frac{dW}{dx}=0;$$
$$C_3: W=\frac{dW}{dx}=U=0; C_4: W=\frac{dW}{dx}=U=V=0 \quad (7)$$

2.2. Ritz functions

In order to satisfy the geometric boundary conditions in Eqs. (6) and (7), the Ritz polynomial functions for approximating displacements are given by (Wang et al. 1995)

$$U=\left(\sum_{i=1}^m p_i x^{i-1}\right)(x)^{P_u^0}(L-x)^{P_u^1}=\sum_{i=1}^m p_i U_i$$
$$V=\left(\sum_{i=1}^m q_i x^{i-1}\right)(x)^{P_v^0}(L-x)^{P_v^1}=\sum_{i=1}^m p_i V_i \quad (8)$$
$$W=\left(\sum_{i=1}^m r_i x^{i-1}\right)(x)^{P_w^0}(L-x)^{P_w^1}=\sum_{i=1}^m p_i W_i$$

where *m* is the number of terms in the Ritz trial functions, p_i, q_i and r_i are the unknown Ritz coefficients to be determined and the powers P_u, P_v and P_w may choose the value as listed in Table 1 to satisfy the simply supported and clamped edge support conditions.

Table 1. Powers of P of Eq.(8)

	Free End	S_1	S_2	S_3	S_4	C_1	C_2	C_3	C_4
P_u	0	0	0	1	1	0	0	1	1
P_v	0	1	0	0	1	1	0	0	1
P_w	0	1	1	1	1	2	2	2	2

The superscripts of *P*, i.e., 0 and 1, denote the cylindrical shell ends at *x*=0 or *x*=*L*, respectively. Ritz polynomial functions are mathematically complete to ensure easy exact differentiation and integration for high accuracy. In the present work, we limit our study to the S_1 and C_4 support conditions as shown in Eqs. (6) and (7).

2.3. Ritz method

In the Ritz method, the Lagrangian functional can be differentiated with respect to each of the unknown Ritz coefficients p_i, q_i and r_i as

$$\left.\begin{aligned}\frac{\partial F}{\partial p_i}&=0\\ \frac{\partial F}{\partial q_i}&=0\\ \frac{\partial F}{\partial r_i}&=0\end{aligned}\right\},\ (\mathrm{i}=1,2,\cdots,\mathrm{m}) \tag{9}$$

Substituting Eq. (8) into Eq. (9), the following equation can be obtained:

$$\left[[K]-\omega^2[M]\right]\{C\}=\{0\} \tag{10}$$

where $[K]$ and $[M]$ are the stiffness and mass matrices of the cylindrical shell, respectively, and $\{C\}=\{p_1,p_2,\cdots,p_m,q_1,q_2,\cdots,r_1,r_2,\cdots,r_m\}^T$ is the column vector containing all Ritz coefficients.

The matrix $[K]$ can be expressed as

$$[K]=\begin{bmatrix}K_{pp} & K_{pq} & K_{pr}\\ K_{pq}^T & K_{qq} & K_{qr}\\ K_{pr}^T & K_{qr}^T & K_{rr}\end{bmatrix} \tag{11}$$

where

$$\begin{aligned}\left(K_{pp}\right)_{ij}&=\frac{Eh}{(1-\nu^2)}\int_0^L\frac{dU_i}{dx}\frac{dU_j}{dx}dx\\ &+\frac{Eh}{2(1+\nu)}\frac{n^2}{R^2}\int_0^L U_iU_jdx+D\left(\frac{1-\nu}{8}\right)\frac{n^2}{R^4}\int_0^L U_iU_jdx\end{aligned} \tag{12}$$

$$\begin{aligned}\left(K_{pq}\right)_{ij}&=-\frac{Eh}{(1-\nu^2)}\frac{n\nu}{R}\int_0^L\frac{dU_i}{dx}V_jdx\\ &+\frac{Eh}{2(1+\nu)}\frac{n}{R}\int_0^L U_i\frac{dV_j}{dx}dx-\frac{3nD}{8R^3}(1-\nu)\int_0^L U_i\frac{dV_j}{dx}dx\end{aligned} \tag{13}$$

$$\begin{aligned}\left(K_{pr}\right)_{ij}&=\frac{Eh}{(1-\nu^2)}\frac{\nu}{R}\int_0^L\frac{dU_i}{dx}W_jdx\\ &+\frac{Dn^2}{2R^3}(1-\nu)\int_0^L U_i\frac{dW_j}{dx}dx\end{aligned} \tag{14}$$

$$\begin{aligned}\left(K_{qq}\right)_{ij}&=\frac{Eh}{(1-\nu^2)}\frac{n^2}{R^2}\int_0^L V_iV_jdx+D\frac{n^2}{R^4}\int_0^L V_iV_jdx\\ &+\frac{Eh}{2(1+\nu)}\int_0^L\frac{dV_i}{dx}\frac{dV_j}{dx}dx+\frac{9D(1-\nu)}{8R^2}\int_0^L\frac{dV_i}{dx}\frac{dV_j}{dx}dx\end{aligned} \tag{15}$$

$$\left(K_{qr}\right)_{ij}=-\frac{Eh}{(1-\nu^2)}\frac{n}{R^2}\int_0^L V_iW_jdx-D\frac{n^3}{R^4}\int_0^L V_iW_jdx \tag{16}$$

$$\begin{aligned}\left(K_{rr}\right)_{ij}&=\frac{Eh}{(1-\nu^2)}\frac{1}{R^2}\int_0^L W_iW_jdx+D\int_0^L\frac{d^2W_i}{dx^2}\frac{d^2W_j}{dx^2}dx\\ &+D\frac{n^4}{R^4}\int_0^L W_iW_jdx-D\frac{n^2}{R^2}\nu\int_0^L\left(\frac{d^2W_i}{dx^2}W_j+W_i\frac{d^2W_j}{dx^2}\right)dx\\ &+2D(1-\nu)\frac{n^2}{R^2}\int_0^L\frac{dW_i}{dx}\frac{dW_j}{dx}dx\end{aligned} \tag{17}$$

$$(i,j=1,2,\cdots,m)$$

and D is the flexural rigidity of the shell and is given by $D=Eh^3/\left[12(1-\nu^2)\right]$.

The matrix $[M]$ is given by

$$[M]=\begin{bmatrix}M_{pp} & 0 & 0\\ 0 & M_{qq} & \\ 0 & 0 & M_{rr}\end{bmatrix} \tag{18}$$

where the elements of the $[M]$ matrix are

$$\left(M_{pp}\right)_{ij}=\rho h\int_0^L U_iU_jdx \tag{19}$$

$$\left(M_{qq}\right)_{ij}=\rho h\int_0^L V_iV_jdx \tag{20}$$

$$\left(M_{rr}\right)_{ij}=\rho h\int_0^L W_iW_jdx \tag{21}$$

$$(i,j=1,2,\cdots,m)$$

3 RITZ METHOD FOR CRACKED SHELLS

The Ritz method is applied to analyze the vibration of a cracked cylindrical shell. Herein the circumferential surface crack is studied and it is modelled as a rotational spring. Two parameters are used to describe the crack damage, i.e.: spring stiffness and location of the crack. The stiffness parameter is related to the crack damage severity. Owing to the introduction of circumferential crack in the shell surface, the shell can be divided into two segments. The strain and kinetic energies in both segments are calculated separately along with the strain energy of the spring. By equating the strain and kinetic energy for both segments along with the strain energy of the spring, the eigenvalue problem is solved to obtain the modal parameters (natural frequency and mode shape) of the cracked circular cylindrical shell.

Spring connection model

The shell is divided into two segments connected by line spring. The strain energy of the cracked shell is given by

$$U=U_1+U_2+U_3 \tag{22}$$

where U is the total strain energy of the shell; U_1 and U_2 are the strain energies of Segments 1 and 2, respectively; U_3 is the strain energy of the connecting springs.

The kinetic energy of the shell is given by

$$T=T_1+T_2 \tag{23}$$

where T is the total kinetic energy of the shell, T_1 and T_2 are the kinetic energies of Segments 1 and 2, respectively. The Lagrangian functional F is the sum

of the strain and kinetic energies of the cracked shell and springs, i.e.

$$F = U + T = U_1 + U_2 + U_3 + T_1 + T_2 \tag{24}$$

The strain energy equation for the connecting springs is

$$U_3 = \int_0^{2\pi} \frac{1}{2} S_{uvw}(u_1 - u_2)^2 Rd\theta \Big|_{x=x_0} + \int_0^{2\pi} \frac{1}{2} S_{uvw}(v_1 - v_2)^2 Rd\theta \Big|_{x=x_0} + \int_0^{2\pi} \frac{1}{2} S_{uvw}(w_1 - w_2)^2 Rd\theta \Big|_{x=x_0} + \int_0^{2\pi} \frac{1}{2} S_s \left(\frac{dw_1}{dx} - \frac{dw_2}{dx}\right)^2 Rd\theta \Big|_{x=x_0} \tag{25}$$

where u_1, v_1, w_1 are displacements in the longitudinal, tangential, and radial directions of Segment 1 and u_2, v_2, w_2 are displacements in the longitudinal, tangential, and radial directions of Segment 2. $S_{uvw} = C_{uvw} Eh^3 / \left[12(1-\nu^2)R^3\right]$ is the translational spring stiffness coefficient to enforce the continuity of *u*, *v* and *w* at the crack location, and C_{uvw} is the non-dimensional spring stiffness parameter. $S_s = C_s Eh^3 / \left[12(1-\nu^2)R\right]$ is the rotational spring stiffness coefficient used at the crack location, and C_s is the non-dimensional spring stiffness parameter that varies the stiffness of the rotational spring connection. C_{uvw} and C_s are related to the depth of the crack and they could be determined by the fracture mechanics. x_0 is the location of the crack along the length direction of the shell.

Applying the Ritz method the following eigenvalue equation can be obtained,

$$\left[[K_{cr}] - \omega_{cr}^2 [M_{cr}]\right]\{C_{cr}\} = \{0\} \tag{26}$$

where $[K_{cr}]$ and $[M_{cr}]$ are the stiffness and mass matrices of the cracked cylindrical shell, and ω_{cr} is the natural frequency of the cracked cylindrical shell.

$\{C_{cr}\} = \{p_{11}, p_{21}, \cdots, p_{m1}, q_{11}, q_{21}, \cdots, q_{m1}, r_{11}, r_{21}, \cdots, r_{m1}, p_{12}, p_{22}, \cdots, p_{m2}, q_{12}, q_{22}, \cdots, q_{m2}, r_{12}, r_{22}, \cdots, r_{m2}\}$ is the column vector of Ritz coefficients.

4 CONTINUOUS WAVELET TRANSFORM

Owing to the presence of the crack in the circular cylindrical shell there will be discontinuities in the mode shapes. The curvature of the mode shape is very effective to detect the abnormal change in the mode shape. However, it is difficult to obtain the accurate mode shape in practice, and the differentiation of deflection will produce more errors. Wavelet transform is an effective tool to detect the discontinuities in a signal and it has been successfully implemented for the damage detection in beams and plates.

A mother wavelet $\psi(x)$ can be identified as a function of zero average value,

$$\int_{-\infty}^{+\infty} \psi(x)dx = 0 \tag{27}$$

and $\psi(x)$ is normalized as:

$$\int_{-\infty}^{+\infty} |\psi(x)|^2 dx = 1 \tag{28}$$

From the mother wavelet $\psi(x)$, the analyzing wavelet can be obtained by dilation parameter *s* and translation parameter *b*:

$$\psi_{b,s}(x) = \frac{1}{\sqrt{s}} \psi\left(\frac{x-b}{s}\right) \tag{29}$$

where both *s* and *b* are real numbers and *s* must be positive.

The continuous wavelet transform of a signal $f(x) \in L^2(R)$ depending on time or space is defined by (Mallat and Hwang, 1992)

$$(Wf)(s,b) = \int_{-\infty}^{+\infty} f(x)\psi^*\left(\frac{x-b}{s}\right)dx \tag{30}$$

where $(*)$ denotes the complex conjugate. The mother wavelet should satisfy an admissibility condition to ensure the existence of the inverse wavelet transform, such as

$$C_\psi = \int_{-\infty}^{+\infty} \frac{|F_\psi(\omega)|^2}{|\omega|} dx < \infty \tag{31}$$

where $F_\psi(\omega)$ denotes the Fourier transform of $\psi(x)$ and is defined as

$$F_\psi(\omega) = \int_{-\infty}^{+\infty} \psi(x) e^{-i\omega x} dx, \ x \in R \tag{32}$$

5 NUMERICAL STUDIES

5.1 Convergence study

To verify the convergence, efficiency and accuracy of the Ritz method in the analysis of circular cylindrical shells, the frequency parameters (Ω) of the intact simply supported (S-S), clamped (C-C) and clamped free (C-F) shells have been compared with the results obtained by Naeem and Sharma (1999). For the sake of comparison, the same shell parameters are used i.e. length-to-radius ratio *L/R*=6, radius-to-thickness ratio *R/h*=500, Poisson's ratio ν=0.3, modulus of elasticity *E*=206832.4MPa and material density ρ=7826.4 kg/m^3. The natural frequency parameter is defined as $\Omega = \omega R\sqrt{\rho(1-\nu^2)/E}$, where

ω is the natural frequency of the circular cylindrical shell. The convergence study results have been presented in Table 2 with circumferential wave number n in the range of 1 and 10. The Ritz polynomial terms have been varied from 2 to 8 to observe the effect on the uncracked natural frequency parameters of the shell. It is observed that the convergence is achieved rapidly with the increase of the Ritz polynomial terms. It is also found that the convergence rate of the method is dependent on the boundary conditions.

Table 2. Convergence of frequency parameters (Ω) of an uncracked simply supported (S-S) shells [L/R=6, R/h=500, v=0.3, E=206832.4 MPa and ρ=7826.4 kg/m^3].

	Number of polynomial terms							
	2		4		6		8	
Circumferential Waves, n	Naeem & Sharma (1999)	Present	Naeem & Sharma (1999)	Present	Naeem & Sharma (1999)	Present	Naeem & Sharma (1999)	Present
1	0.15038	0.15038	0.14067	0.14067	0.14064	0.14064	0.14064	0.14064
2	0.05972	0.05971	0.05434	0.05434	0.05432	0.05432	0.05432	0.05432
3	0.02997	0.02996	0.02707	0.02708	0.02707	0.02707	0.02707	0.02707
4	0.01934	0.01934	0.01778	0.01777	0.01778	0.01777	0.01778	0.01777
5	0.01780	0.01779	0.01709	0.01707	0.01709	0.01707	0.01709	0.01707
6	0.02159	0.02160	0.02130	0.02130	0.02130	0.02130	0.02130	0.02130
7	0.02821	0.02820	0.02809	0.02808	0.02809	0.02808	0.02809	0.02808
8	0.03652	0.03653	0.03647	0.03647	0.03647	0.03647	0.03647	0.03647
9	0.04620	0.04620	0.04617	0.04617	0.04617	0.04617	0.04617	0.04617
10	0.05711	0.05710	0.05709	0.05709	0.05709	0.05709	0.05709	0.05709

Table 3. Comparison of the frequency parameters (Ω) for simply supported (S-S), clamped (C-C) and clamped-simply (C-S) supported cylindrical shells [L/R=20, h/R=0.01, v=0.3, E=206832.4 MPa, ρ=7826.4 kg/m^3 and Ritz polynomial terms=6].

	S-S			C-C			C-S		
Circumferential Wave, n	Loy et al. (1997)	Zhang et al. (2001)	Present	Loy et al. (1997)	Zhang et al. (2001)	Present	Loy et al. (1997)	Zhang et al. (2001)	Present
1	0.01610	0.01610	0.01610	0.03289	0.03488	0.03342	0.02397	0.02472	0.02416
2	0.00938	0.00938	0.00938	0.01393	0.01405	0.01400	0.01123	0.01128	0.01124
3	0.02211	0.02211	0.02210	0.02267	0.02273	0.02267	0.02231	0.02234	0.02231
4	0.04210	0.04210	0.04209	0.04221	0.04227	0.04221	0.04214	0.04217	0.04214
5	0.06801	0.06801	0.06801	0.06805	0.06812	0.06805	0.06802	0.06805	0.06802

5.2 Numerical verification of results

To verify the accuracy of the present analysis the results are compared with those available in the literature. In Table 3 the natural frequency parameters of uncracked shells with simply supported (S-S), clamped (C-C) and clamped-simply supported (C-S) boundary conditions have been compared with the results of Loy et al. (1997) and Zhang et al. (2001). The parameters used for the analysis are: length-to-radius ratio of the circular cylindrical shell L/R=20, thickness-to-radius ratio h/R=0.01 and the number of Ritz polynomial terms being 6.

From Table 3, it is observed that the natural frequency parameters agree well with those obtained by Loy et al. (1997) and Zhang et al. (2001), indicating the accuracy of the present method. The percentage difference is listed in Table 4. For circumferential wave n=1, simply supported, clamped and clamped-simply supported circular cylindrical shells have the differences in natural frequency parameters for the above mentioned studies and are 0.000 & 0.000, -1.627 & 4.183, -0.763 & 2.281 percentage, respectively. For the clamped case the difference is higher than usual but in the other cases it is less than 1% which is lower than the limits of engineering tolerance. For higher values of circumferential wave number i.e. n=2 to 5, the differences in frequency parameters are less than 1 % for all the boundary conditions as can be seen in Table 4. It is clearly indicated that the method is efficient and accurate to produce satisfactory results for the vibration analysis of thin circular cylindrical shells.

Table 4. Differences (%) of frequency parameters (Ω) between the present study and the results obtained by Loy et al. (1997) and Zhang et al. (2001) as shown in Table 3.

	S-S		C-C		C-S	
Circumferential Wave, *n*	Loy et al. (1997)	Zhang et al. (2001)	Loy et al. (1997)	Zhang et al. (2001)	Loy et al. (1997)	Zhang et al. (2001)
1	0.000	0.000	-1.627	4.183	-0.763	2.281
2	0.053	0.053	-0.423	0.434	-0.134	0.363
3	0.014	0.014	0.000	0.233	0.009	0.121
4	0.005	0.005	0.002	0.151	0.005	0.069
5	0.003	0.003	0.001	0.104	0.001	0.046

Table 5. Vibration frequencies (Ω) of the uncracked circular cylindrical shell [h=0.05m, R=1m, v=0.3, E=206832.4MPa and ρ=7826.4 kg/m^3].

Boundary Conditions		Circumferential Wave Number, *n*				
	L/R	1	2	3	4	5
S-S	1	0.59162	0.67687	0.54120	0.49575	0.54518
	5	0.18639	0.08695	0.12019	0.21609	0.34506
	10	0.05911	0.04454	0.11105	0.21127	0.34087
	15	0.02795	0.04016	0.11009	0.21053	0.34013
	20	0.01610	0.03916	0.10980	0.21027	0.33986
S-C	1	0.87647	0.70554	0.58744	0.55390	0.60122
	5	0.21242	0.11133	0.12736	0.21817	0.346000
	10	0.08009	0.05022	0.11181	0.211513	0.34099
	15	0.04065	0.04165	0.11028	0.21060	0.34017
	20	0.02416	0.03979	0.10988	0.21031	0.33990
C-C	1	0.91126	0.74475	0.64739	0.62386	0.66854
	5	0.24179	0.13627	0.13703	0.22099	0.34714
	10	0.10117	0.05825	0.11294	0.21181	0.34114
	15	0.05451	0.04408	0.11055	0.210684	0.34022
	20	0.03343	0.04067	0.10998	0.21034	0.33992
C-F	1	0.56254	0.35805	0.27078	0.28971	0.38879
	5	0.07649	0.04885	0.11140	0.21093	0.34012
	10	0.02243	0.03966	0.10981	0.21014	0.33963
	15	0.01031	0.03897	0.10962	0.21002	0.33957
	20	0.00590	0.03882	0.10952	0.20994	0.33953

5.3 Vibration analysis of uncracked cylindrical shells

The vibration analysis program developed for this study has been used to determine the fundamental circumferential mode frequencies of different shell models. The data furnished by this model has been compared with the ones by the cracked shell models to determine the effect of the circumferential surface crack upon the fundamental circumferential mode frequencies of the specific shell system.

In Table 5 different combinations of boundary conditions have been analysed with different circumferential wave numbers (n) to show the gradual changes in natural frequency in the shell system. The shells are analysed with different length-to-radius ratios (L/R), a shell thickness of h=0.05m and a shell radius of R=1m. The boundary conditions that have been used for the analysis are simply supported (S-S), simply support-clamped (S-C), clamped-clamped (C-C) and clamped-free (C-F). From Table 5 it is observed that the frequencies of circular cylindrical shells are affected by different length-to-radius ratio (L/R), the circumferential wave number (n) and boundary conditions. The frequencies decrease with the increase of the length-to-radius (L/R) ratio and increase with the increase of the circumferential wave number (n). Different combinations of boundary conditions also affect the frequencies. It can be seen from Table 5 that shells with clamped-clamped (C-C) boundary condition has higher frequencies than the ones with other boundary conditions. However, the boundary condition effect diminishes with the increasing circumferential wave number (n).

5.4 Vibration analysis of cracked cylindrical shells

The above model is used for modelling the surface cracks on the shell. The different damage severities are simulated by varying the rotational spring stiffness. The program has been developed with an option to change the line spring's position along the length of the cylindrical shell. In Table 6 the natural frequency parameters (Ω_{cr}) of cracked circular cylindrical shells with different combinations of boundary conditions, length-to-radius ratio (L/R) and C_s values are presented. The crack has been simulated by line spring connections along the circumference in the middle (0.5L) of the shell. From Table 6 it can be observed that the change in the natural frequency parameters (Ω_{cr}) of the cracked cylindrical shells is very small even though the length-to-radius ratio (L/R) is 15. The change is almost negligible when the length-to-radius ratio is smaller than 15 (1 to 10). But some abrupt changes are observed for clamped (C-C) and simply support-clamped (S-C) cylindrical shells when the length to radius ratio L/R is 20.

Table 6. Natural frequency parameters (Ω_{cr}) of cracked circular cylindrical shells with different values of C_s; crack position in the middle (0.5L) of the shell.
[h=0.05m, R=1m, v=0.3, C_{uvw}=10^7, n=1, E=206832.4 MPa and ρ=7826.4 kg/m^3]

		Rotational Spring Stiffness Parameter, C_s										
Boundary Conditions	L/R	10^{-3}	10^{-2}	10^{-1}	1	10	10^2	10^3	10^4	10^5	10^6	10^7
S-S	1	0.59157	0.59157	0.59157	0.59157	0.59157	0.59157	0.59157	0.59157	0.59157	0.59157	0.59157
	5	0.18638	0.18638	0.18638	0.18638	0.18638	0.18638	0.18638	0.18638	0.18638	0.18638	0.18638
	10	0.05911	0.05911	0.05911	0.05911	0.05911	0.05911	0.05911	0.05911	0.05911	0.0591	0.05911
	15	0.02795	0.02795	0.02795	0.02795	0.02795	0.02795	0.02795	0.02795	0.02795	0.02795	0.02795
	20	0.01610	0.01610	0.01610	0.01610	0.01610	0.01610	0.01610	0.01610	0.01610	0.01610	0.01610
C-C	1	0.88208	0.88218	0.88315	0.89019	0.90528	0.91052	0.91117	0.91124	0.91125	0.91125	0.91125
	5	0.24114	0.24114	0.24114	0.24114	0.24114	0.24114	0.24114	0.24114	0.24114	0.24114	0.24114
	10	0.10022	0.10022	0.10022	0.10022	0.10024	0.10025	0.10026	0.10026	0.10026	0.10026	0.10028
	15	0.05395	0.05395	0.05395	0.05395	0.05395	0.05396	0.05397	0.05397	0.05397	0.05397	0.05397
	20	0.03314	0.03314	0.03314	0.03314	0.03314	0.03315	0.0331505	0.03315	0.03315	0.14350	0.10429
S-C	1	0.86005	0.86011	0.86070	0.86490	0.87332	0.87609	0.87643	0.87646	0.87646	0.87646	0.87646
	5	0.21199	0.21199	0.21199	0.21199	0.21199	0.21199	0.21199	0.21199	0.21199	0.21199	0.21199
	10	0.07967	0.08010	0.07965	0.07964	0.07964	0.07968	0.07970	0.07958	0.07954	0.07963	0.07964
	15	0.04071	0.04060	0.04021	0.04032	0.04062	0.04047	0.04043	0.04054	0.04040	0.04097	0.04046
	20	0.02035	0.02483	0.02389	0.02238	0.02309	0.02208	0.02190	0.02456	0.02243	0.02245	0.02270
C-F	1	0.56182	0.56182	0.56184	0.56201	0.56235	0.56248	0.56249	0.56250	0.56250	0.56250	0.56250
	5	0.07608	0.07608	0.07608	0.07608	0.07608	0.07608	0.07608	0.07608	0.07608	0.07608	0.07608
	10	0.02230	0.02230	0.02230	0.02230	0.02230	0.02230	0.02230	0.02230	0.02230	0.02230	0.02230
	15	0.01027	0.01027	0.01027	0.01027	0.01027	0.01028	0.01028	0.01028	0.01028	0.01028	0.01028
	20	0.00585	0.00585	0.00585	0.00585	0.00585	0.00585	0.00586	0.00586	0.00586	0.00586	0.00586

To determine a meaningful scale for the rotational spring stiffness parameter C_s, an analysis is conducted for the C_s parameter, and the results are listed in Table 7. For different boundary conditions, the natural frequency parameter gradually changes as the rotational spring stiffness parameter varies. The rotational spring stiffness parameter values are between 10^{-3} and 10^7. As seen from Table 7, the natural frequency parameter remains unchanged when the rotational spring stiffness parameter value is between 10^2 and 10^7. It is indicated that any value from 10^2 to 10^7 can be selected for the rotational spring stiffness parameter C_s for simulating different damage severities because it is assumed that in real cases damage will cause more rotation in the radial direction of the cylindrical shell without changing its natural frequency much.

By setting the rotational spring stiffness coefficient (C_s) to zero, it represents a case where there is no resistance between the rotations of the two segments. Table 8 lists the hinged vibration frequency and effects of different locations, for all shell systems analysed in this study. It is clearly shown from Table 8 that except for simply supported shells the hinged vibration frequencies are always less than the uncracked vibration frequencies of the circular cylindrical shell.

Table 7. Natural frequency parameters (Ω_{cr}) of cracked shell subjected to different boundary conditions and with different spring stiffness parameter [n=1, L=2m, h=0.005m, R=0.1m, v=0.3, E=206832.4 MPa, ρ=7826.4 kg/m^3, C_{uvw}=10^7, polynomial terms=6 and crack position=0.5L].

	Rotational Spring Stiffness Parameter, C_s										
Boundary Conditions	10^{-3}	10^{-2}	10^{-1}	1	10	10^2	10^3	10^4	10^5	10^6	10^7
S-S	0.01610	0.01610	0.01610	0.01610	0.01610	0.01610	0.01610	0.01610	0.01610	0.01610	0.01610
C-C	0.03314	0.03314	0.03314	0.03314	0.03314	0.03315	0.03315	0.03315	0.03315	0.03315	0.03315
S-C	0.02407	0.02407	0.02407	0.02407	0.02407	0.02407	0.02407	0.02407	0.02407	0.02407	0.02407
C-F	0.00585	0.00585	0.00585	0.00585	0.00585	0.00585	0.00586	0.00586	0.00586	0.00586	0.00586

Effect of crack and its location on natural frequency of circular cylindrical shell

To study the effect of the crack and its location on the fundamental mode frequencies of the circular cylindrical shell, the shell is analysed with an intermediate rotational spring stiffness parameter value of C_s=10^3. The results of the analysis are shown in Table 9. From the results it is obvious that the crack doesn't have any significant effect on the fundamental mode frequencies of the simply supported cylindrical shell as the difference in frequency parameters for all crack locations is 0.00%. For clamped (C-C), simply supported-clamped (S-C) and clamped-free (C-F) cylindrical shells the cracked frequencies are always smaller than the uncracked fundamental mode frequencies.

The frequency changes due to the introduction of the crack on the shell surface is too small to be used as a tool for detecting the damage position as can be observed from Tables 8 and 9. However, it still provides evidence of the presence of an imperfection in the system. Because natural frequencies are insensitive to crack damage, a special focus has been given on mode shape analysis for damage detection for cylindrical shells.

Table 8. Effect of hinge connections upon the uncracked fundamental mode frequency of various shell systems [n=1, L=2m, h=0.005m, R=0.1m, v=0.3, E=206832.4 MPa, ρ=7826.4 kg/m^3, C_{uvw}=10^7 and C_s=0].

Boundary Conditions	Uncracked Frequency(Ω)	Hinge Location				
		0.1	0.2	0.3	0.4	0.5
S-S	0.01610	0.01610	0.01610	0.01610	0.01610	0.01610
		0.00%	0.00%	0.00%	0.00%	0.00%
C-C	0.03343	0.03317	0.03313	0.03313	0.03314	0.03314
		-0.78%	-0.90%	-0.90%	-0.87%	-0.87%
S-C	0.02416	0.02415	0.02413	0.02411	0.02409	0.02407
		-0.04%	-0.12%	-0.21%	-0.29%	-0.37%
C-F	0.00587	0.00584	0.00584	0.00584	0.00585	0.00585
		-0.51%	-0.51%	-0.51%	-0.34%	-0.34%

Note: Frequency parameter (frequency change in percentage)

Table 9. Effect of crack upon the uncracked fundamental mode frequency of various shell system [n=1, L=2m, h=0.005m, R=0.1m, v=0.3, E=206832.4 MPa, ρ=7826.4 kg/m^3, C_{uvw}=10^7 and C_s=10^3].

Boundary Conditions	Uncracked Frequency(Ω)	Crack Location				
		0.1	0.2	0.3	0.4	0.5
S-S	0.01610	0.01610	0.01610	0.01610	0.01610	0.01610
		0.00%	0.00%	0.00%	0.00%	0.00%
C-C	0.03343	0.03318	0.03313	0.03314	0.03315	0.03315
		-0.75%	-0.90%	-0.87%	-0.84%	-0.84%
S-C	0.02416	0.02415	0.02413	0.02411	0.02409	0.02407
		-0.04%	-0.12%	-0.21%	-0.29%	-0.37%
C-F	0.00587	0.00584	0.00584	0.00585	0.00585	0.00586
		-0.51%	-0.51%	-0.34%	-0.34%	-0.17%

Note: Frequency parameter (frequency change in percentage)

6 DAMAGE DETECTION USING WAVELET ANALYSIS

A mode shape is a specific pattern of vibration of a structural system at a specific frequency. In this analysis the eigenvectors associated with the first vibration mode is used to determine the first mode shape. The mode shape has been used as the analysed signal for the wavelet analysis for locating the damage position. The parameters used in the analysis are: circumferential wave number n=1, shell length L=2m, shell thickness h=0.005m, shell radius R=0.1m, Poisson's ratio v=0.3, modulus of elasticity E=206832.4 MPa, material density ρ=7826.4 kg/m^3, rotational spring stiffness parameter C_s=10^{-3} to 10^{4}and spring stiffness parameter C_{uvw}=10^7. The rotational spring stiffness parameter has been varied up to a certain limit to examine its sensitivity on the wavelet analysis. The reason for the selection of rotational spring stiffness parameter C_s =10^4 is to create a larger difference in the stiffness of the continuity condition and rotation of the circular cylindrical shell. For wavelet analysis the daubechies wavelet (db-10) is used to find the discontinuity in the shell system.

6.1 Simply supported shell with one crack

For the wavelet analysis the mode shape has been used as the analysed signal for all the cases presented here. The daubechies wavelet (db-10) has been used for finding the discontinuity in the shell system. The rotational spring stiffness parameter (C_s) is varied from 10^{-3} to 10^4 to simulate different crack severity on the circular cylindrical shell at the position of 0.3L. It can be seen from Figure 2 that the wavelets can identify the damage position in the simply supported shell system by analyzing its mode shape at different rotational spring stiffness (C_s) values.

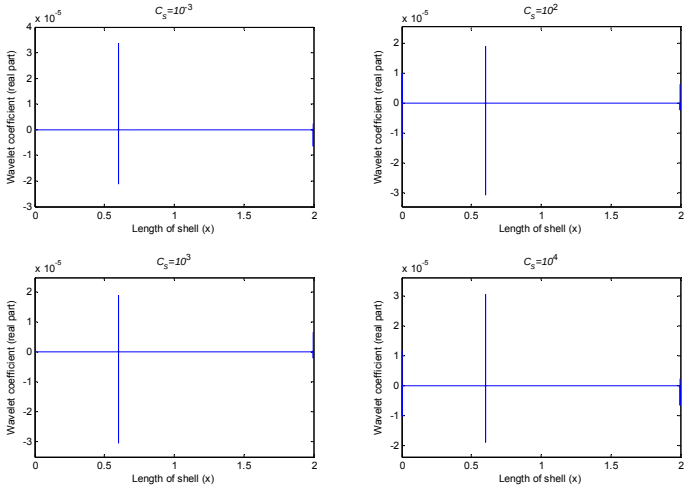

Figure 2. Wavelet analysis of simply supported shell with a crack at 0.3L with different C_s values.

6.2 Clamped shell with one crack

To verify the effectiveness of wavelet transform in the detection of the damage location in the shell system, in this section a crack has been simulated in the clamped shell at the position of 0.3L. From Figure 3 it is quite clear that wavelet transform is capable of detecting the damage in the clamped shell when the damage is located at the 0.3L position of the shell. The jumps in the graphs in all the cases prove that different values of rotational spring stiffness parameter (C_s) have no effect on the wavelet transform.

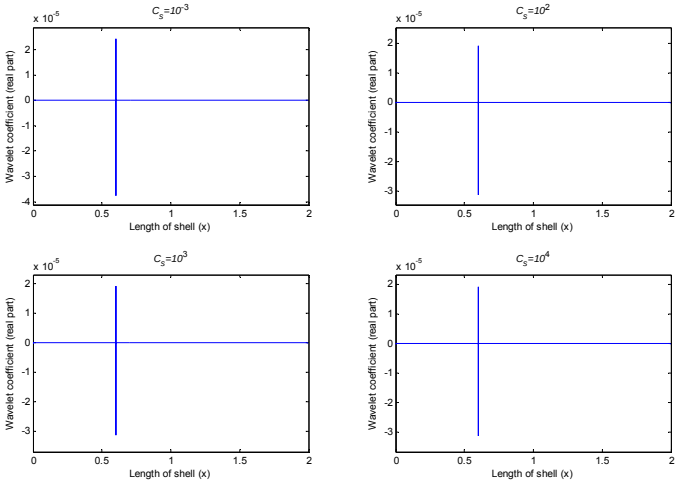

Figure 3. Wavelet analysis of clamped shell with a crack at 0.3L with different C_s values.

6.3 Clamped-free shell with one crack

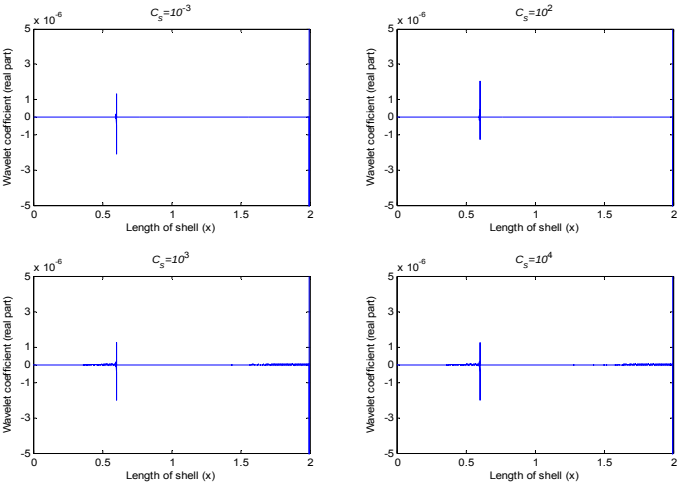

Figure 4. Wavelet analysis of clamped-free shell with a crack at 0.3L with different C_s values.

Similarly wavelet analysis is also conducted for clamped-free boundary condition with a crack at 0.3L in the circular cylindrical shell with the same parameters as in the case of simply supported and clamped shells. The results are presented in Figure 4. It is clearly seen that for the crack position of 0.3L in the circular cylindrical shell the crack location can be identified by the wavelet transform for all C_s val-

ues. The crack location is barely identifiable when the C_s value is 10^3 and the crack location cannot be identified for a C_s value of 10^4. Thus the clamped-free shell shows a similar behaviour as the simply supported shell when the crack damage is presented at 0.3L in the circular cylindrical shell.

6.4 Simply supported and clamped shells with two cracks

To check the effectivity of the method for the shell system with multiple cracks, the shell has been analysed with two cracks. By using the same parameters as discussed in the previous sections, the shell has been analysed for both simply supported and clamped conditions with only a rotational spring stiffness (C_s) parameter value of 10^3. The results are demonstrated in Figures 5 and 6. It is clearly seen from the figures that there are two peaks in the shell system at the crack positions. It is proved that the method is applicable for the shell system with multiple cracks.

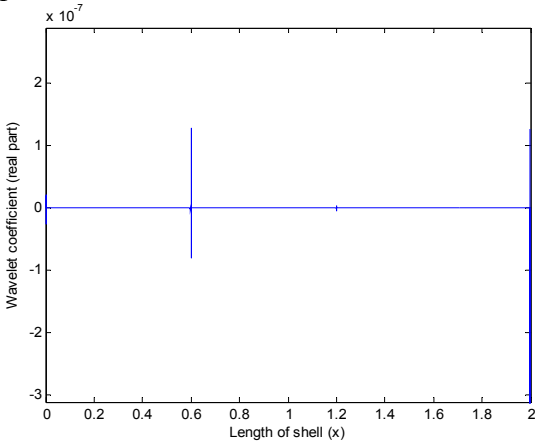

Figure 5. Wavelet analysis result for simply supported cylindrical shell with two cracks at 0.3L and 0.6L positions. (L=2m, h=0.005m, R=0.1m, v=0.3, E=206832.4 MPa, ρ=7826.4 kg/m^3, C_{uvw}=10^7 and C_s =10^3).

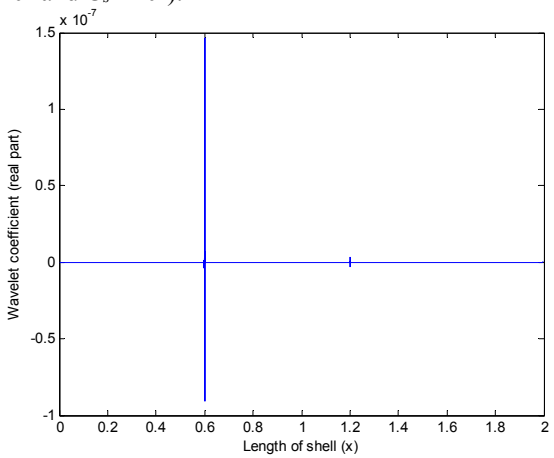

Figure 6. Wavelet analysis result for clamped cylindrical shell with two cracks at 0.3L and 0.6L positions. (L=2m, h=0.005m, R=0.1m, v=0.3, E=206832.4 MPa, ρ=7826.4 kg/m^3, C_{uvw}=10^7 and C_s =10^3).

6.5 Wavelet analysis with noise

Considering the practical condition of vibration measurements the shell is also analysed with noise. White noise is added to the calculated responses of the shell to simulate the polluted measurements. The wavelet analysis is then carried out with the simulated noisy measurements to see the effect of both the crack and noise on the effectiveness of the wavelet transform. For simulating the noise the formula used is (Zhu and Law, 2006)

$$w = w_{calculated} + E_p N_{oise} \sigma(w_{calculated}) \tag{33}$$

where w is the polluted displacement, E_p is the noise level, N_{oise} is a standard normal distribution vector with a zero mean value and a unit standard deviation, $w_{calculated}$ is the calculated displacement, and $\sigma(w_{calculated})$ is the standard deviation for the calculated displacements. The noise level E_p has been taken as 0.01% in this study as higher noise level makes the wavelet transform insensitive to the damage.

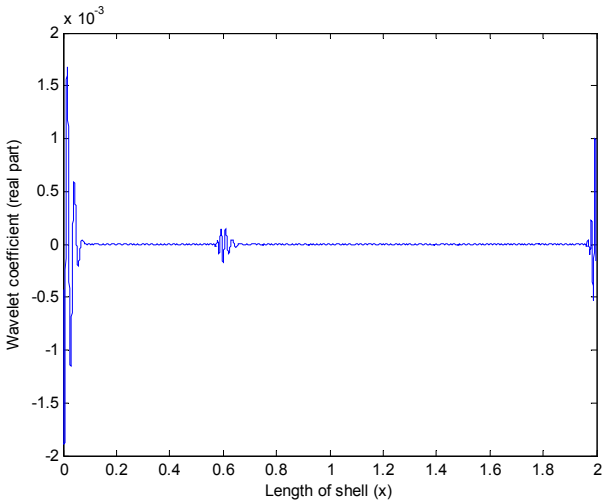

Figure 7. Wavelet analysis result with noise for simply supported cylindrical shell with a crack at 0.3L. (L=2m, h=0.005m, R=0.1m, v=0.3, E=206832.4 MPa, ρ=7826.4 kg/m^3, C_{uvw}=10^7, C_s =10^3, E_p =0.01% and wavelet coefficient scale =64)

The rotational spring stiffness parameter C_s is taken as 10^3. The results of the wavelet analysis with noise of simply supported and clamped shells with a crack located at 0.3L are shown in Figures 7 and 8. The wavelet coefficient of the displacement (w) of the circular cylindrical shell with a scale of 64 are used for all the cases. As can be seen from Figures 7 and 8, wavelet transform of the displacement (w) of the circular cylindrical shell can detect the damage position successfully with a noise level of 0.01%. The distinctive peak on the curve is the damage location for the shells.

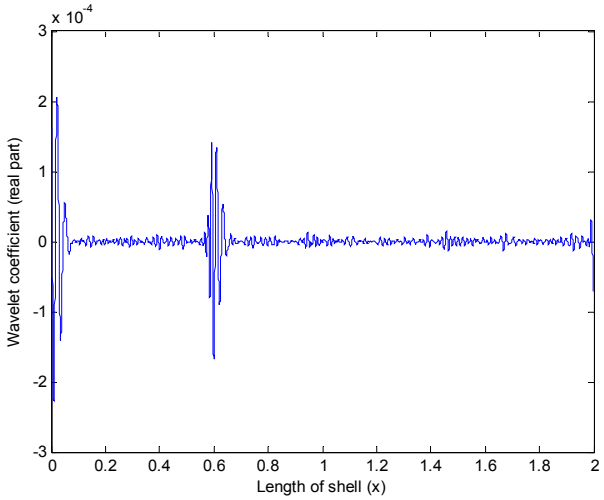

Figure 8. Wavelet analysis result with noise for clamped cylindrical shell with a crack at 0.3L. (L=2m, h=0.005m, R=0.1m, v=0.3, E=206832.4 MPa, ρ=7826.4 kg/m^3, C_{uvw}=10^7, C_s =10^3, E_p =0.01% and wavelet coefficient scale=64)

7 CONCLUSIONS

A model based damage detection method for circular cylindrical shells has been proposed based on the Ritz method. The crack on the shell surface has been modelled by the line spring. Natural frequency and mode shape have been analysed with different combination of boundary conditions to assess the effect of circumferential surface crack on these modal parameters. The natural frequency changes with different position of the circumferential crack along the shell length are very minimal and cannot be used for damage detection. Wavelet analysis has been carried out to determine the discontinuities of the mode shape with different crack positions along the shell length direction. From the results of the wavelet analysis it can be concluded that damage in the circular cylindrical shell can be detected successfully by the proposed model based damage detection method.

8 REFERENCES

Brownjohn, J. M. W., "Structural Health Monitoring of Civil Infrastructure," *Philosophical Transactions: Mathematical, Physical and Engineering Sciences*, Vol.365, No.1851, 2007, pp.589-622.

Chondros, T. G., Dimarogonas, A. D. and Yao, J., "A Continuous Cracked Beam Vibration Theory," *Journal of Sound and Vibration*, Vol.215, No. 1, 1998, pp.17-34.

Dimarogonas, A. and Massouros, G., "Torsional Vibration of a Shaft with a Circumferential Crack," *Engineering Fracture Mechanics*, Vol.15, No. 3-4, 1981, pp.439-444.

Doebling, S. W., Farrar, C. R. and Prime, M. B., "A Summary Review of Vibration-Based Damage Identification Methods," *Shock and Vibration Digest*, Vol.30, No.2, 1998, pp.91-105.

Fernandez-Saez, J., Rubio, L. and Navarro, C., "Approximate Calculation of the Fundamental Frequency for Bending Vibrations of Cracked Beams," *Journal of Sound and Vibration*, Vol.225, No.2, 1999, pp.345-352.

Javidruzi, M., Vafai, A., Chen, J. F. and Chilton, J. C., "Vibration, Buckling and Dynamic Stability of Cracked Cylindrical Shells," *Thin-Walled Structures*, Vol.42, No.1, 2004, pp.79-99.

Law, S. S., Li, X. Y., Zhu, X. Q. and Chan, S. L., "Structural Damage Detection from Wavelet Packet Sensitivity," *Engineering Structures*, Vol.27, No.9, 2005, pp.1339-1348.

Lee, U. and Kim, S., "Identification of Multiple Directional Damages in a Thin Cylindrical Shell," *International Journal of Solids and Structures*, Vol.43, No.9, 2006, pp.2723-2743.

Leissa, A. W., *Vibration of Shells*, Scientific and Technical Information Office, National Aeronautics and Space Administration, Washington, 1973.

Loy, C. T., Lam, K. Y. and Shu, C., "Analysis of Cylindrical Shells Using Generalized Differential Quadrature," *Shock and Vibration*, Vol.4, No.3, 1997, pp.193-198.

Lu, C.-J. and Hsu, Y.-T., "Vibration Analysis of an Inhomogeneous String for Damage Detection by Wavelet Transform," *International Journal of Mechanical Sciences*, Vol.44, No.4, 2002, pp.745-754.

Mohan, R., "Fracture Analyses of Surface-Cracked Pipes and Elbows Using the Line-Spring/Shell Model," *Engineering Fracture Mechanics*, Vol.59, No.4, 1998, pp.425-438.

Naeem, M. N. and Sharma, C. B., "Prediction of Natural Frequencies for Thin Circular Cylindrical Shells," *Proceedings of the Institution of Mechanical Engineers, Part C: Journal of Mechanical Engineering Science*, Vol.214, No.10, 2000, pp.1313-1328.

Rajasekaran, S. and Varghese, S. P., "Damage Detection in Beams and Plates Using Wavelet Transforms," *Computers and Concrete*, Vol.2, No.6, 2005, pp.481-498.

Rice, J. R. and Levy, N., "The Part-Through Surface Crack in an Elastic Plate," *Journal of Applied Mechanics ASME*, Vol.39, No.1, 1972, pp.185-194.

Roytman, A. and Titova, O., "An Analytical Approach to Determining the Dynamic Characteristics of a Cylindrical Shell with Closing Cracks," *Journal of Sound and Vibration*, Vol.254, No.4, 2002, pp.379-386.

Sarker L., Xiang Y., Uy B. and Zhu X. Q., "Damage detection of circular cylindrical shells by Ritz method," *Journal of Physics: Conference Series*, Vol. 305, No.1, 2011, 012117.

Sobel, L. H., "Effects of Boundary Conditions on the Stability of Cylinders Subject to Lateral and Axial Pressures," *AIAA Journal*, Vol.2, No.8, 1964, pp.1437-1440.

Sohn, H., Czarnecki, J. A. and Farrar, C. R., "Structural Health Monitoring Using Statistical Process Control," *Journal of Structural Engineering ASCE*, Vol.126, No.11, 2000pp.1356-1363.

Swaddiwudhipong, S., Tian, J. and Wang, C. M., "Vibrations of Cylindrical Shells with Intermediate Supports," *Journal of Sound and Vibration*, Vol.187, No.1, 1995, pp.69-93.

Yan, Y. J. and Yam, L. H., "Online Detection of Crack Damage in Composite Plates Using Embedded Piezoelectric Actuators/Sensors and Wavelet Analysis," Composite Structures, Vol.58, No.1, 2002, pp.29-38.

Yan, Y. J., Cheng, L., Wu, Z. Y. and Yam, L. H., "Development in Vibration-based Structural Damage Detection Technique," *Mechanical Systems and Signal Processing*, Vol.21, No.5, 2007, pp.2198-2211.

Yokoyama, T. and Chen, M. C., "Vibration Analysis of Edge-cracked Beams Using a Line-spring Model," *Engineering Fracture Mechanics*, Vol.59, No.3, 1998, pp.403-409.

Zhang, L., Xiang, Y. and Wei, G. W., "Local Adaptive Differential Quadrature for Free Vibration Analysis of Cylindrical Shells with Various Boundary Conditions," *International Journal of Mechanical Sciences*, Vol.48, No.10, 2006, pp.1126-1138.

Zhang, X. M., Liu, G. R. and Lam, K. Y., "Vibration Analysis of Thin Cylindrical Shells Using Wave Propagation Approach," *Journal of Sound and Vibration*, Vol. 239, No.3, 2001, pp. 397-403.

Zhang Y., Lie S. T., Xiang Z. H. and Lu Q.H., "A frequency shift curve based damage detection method for cylindrical shell structures," *Journal of Sound and Vibration*, Vol. 333, No. 6, 2014, 1671-1683.

Zhu, X. Q. and Law, S. S., "Wavelet-Based Crack Identification of Bridge Beam from Operational Deflection Time History," *International Journal of Solids and Structures*, Vol.43, No.7-8, 2006, pp.2299-2317.

Zhu, X., Li, T. Y., Zhao, Y. and Yan, J., "Vibrational Power Flow Analysis of Thin Cylindrical Shell with a Circumferential Surface Crack," *Journal of Sound and Vibration*, Vol.302, No.1-2, 2007, pp.332-349.